

## Electrochemical Studies of Titanium and its Ti-6Al-4V Alloy in Phosphoric Acid Solutions

A.A. Ghoneim\*, A.S. Mogoda, Kh.A. Awad, F. El-Taib Heikal

Department of Chemistry, Faculty of Science, Cairo University, Giza 12613, Egypt

\*E-mail: [Azzaghoneim@gmail.com](mailto:Azzaghoneim@gmail.com)

Received: 13 May 2012 / Accepted: 8 June 2012 / Published: 1 July 2012

---

The influence of phosphoric acid concentration and temperature on the electrochemical behavior of pure Ti and Ti-6Al-4V alloy was investigated using electrochemical techniques. The open circuit potential (OCP) and electrochemical impedance results over a wide range of concentration (1.0-14 M) showed that Ti appears more corrosion resistant than its alloy. Two different types of behavior were observed for Ti and its alloy, in the concentration range up to 4.0M for Ti and 3.0M for the alloy, the OCP exhibits initial positive shift in potential associated with thickening of the oxide film formed on the material surface, after that and as the acid concentration is increased to higher values, the potential changes towards more negative values due to its thinning and dissolution. The electrochemical impedance spectroscopy (EIS) confirms this trend as can be identified by the values of the resistance  $R_{ox}$  and the oxide thickness  $1/c_{ox}$ . On the other hand, at any given temperature, titanium exhibits higher thickening rate ( $\delta / \text{nm decade}^{-1}$ ) for its oxide film growth in 1.0 M  $\text{H}_3\text{PO}_4$  medium.

---

**Keywords:** Titanium, Ti-6Al-4V alloy, passivation, EIS measurements,  $\text{H}_3\text{PO}_4$  solutions.

### 1. INTRODUCTION

Titanium and its alloys have over the years proven themselves to be technically superior and cost effective materials for a wide range of applications spanning the industries of aerospace, power generation equipments, and even commercial products [1]. The noticeable attractive properties of titanium alloys have facilitated in their selection and enhanced use in marine and a spectrum of other performance-critical applications [2]. Metallic materials are being increasingly used in medical applications as implants to restore lost functions or replace organs functioning below acceptable levels. Titanium alloys are among the most used metallic biomaterials, particularly for orthopaedic applications [3]. They possess a set of suitable properties for these applications such as low specific weight, high corrosion resistance and biocompatibility. Titanium is immune from corrosive attack in

salty water or marine atmosphere where conventional materials often fail. It exhibits exceptional resistance to a broad range of acids, alkalis, natural waters and industrial chemicals [4-6]. The corrosion resistance is determined by the formation of an adherent thin titanium oxide layer on the surface of titanium or a titanium alloy. This film mainly consists of  $\text{TiO}_2$  [7]. The film functions as a barrier to the tendency of the metal to interact with corrosive media. Several authors [8-13] made electrochemical investigations of titanium and its alloys in different concentrations of  $\text{H}_3\text{PO}_4$  at room or elevated temperatures. The critical current density and passive current density of commercially pure titanium in 1 mol/L  $\text{H}_3\text{PO}_4$  were found to increase with the increase of temperature [8].

It was found previously [14] that the addition of alloying elements such as Al, V, Mo, Nb to Ti increase the steady dissolution current in the passive state, through a change of defectness degree of passive films when the alloying atoms enter its lattice.

In the case of Ti-6Al-4V, it had been reported in the literature [15] that the vanadium oxide formed on the surface of Ti-6Al-4V alloy dissolves. Dissolution of vanadium oxide results in the generation and diffusion of vacancies in the oxide layer of Ti-6Al-4V. Hence, vanadium as an alloying element could not contribute to improvement of the surface film on Ti-6Al-4V alloy. It was also reported that titanium has a higher resistance to corrosion compared to its Ti-6Al-4V alloys in different media including, chloride [16], oxalic acid [17], low and highly concentrated HBr solutions [18]. Also, in simulated body condition (Hanks solution) [19] and in artificial saliva [20, 21]. Recently, we studied the corrosion and passivation behaviour of Ti and Ti-6Al-4V alloy in azide and halide solutions [22]. The results showed that increasing azide concentration decreases the spontaneous thickening rates of the passive oxide film on each sample and increases the rate of corrosion. Also, it was found that Ti has a stronger tendency to form oxide layers in bromide more than in azide and other halide media,

Accordingly this work aims at studying the behavior of pure Ti metal relative to its Ti-6Al-4V alloy in phosphoric acid solutions over a wide concentration range from 1.0 to 14 M. The effect of temperature was also examined in 1.0 M  $\text{H}_3\text{PO}_4$  solution using electrochemical techniques.

## 2. MATERIALS AND METHODS

The working electrodes were made from spectroscopically pure titanium and Ti-6Al-4V alloy with composition in wt% of: 5.70Al, 3.85V, 0.18Fe, 0.038C, 0.106O, 0.035N. The electrodes were supplied in the form of massive cylindrical rods from Johnson and Maltby (England). The electrodes give always a fixed exposed surface area of 0.196 and 0.384  $\text{cm}^2$  for titanium and titanium alloy, respectively throughout the whole measurements. The electrode surfaces were mechanically polished using finer grades of emery papers (600-1200 grade). The test solutions were prepared from analar grade (BDH) phosphoric acid by appropriate dilution using triple distilled water. The cell used was a typical three-electrode one fitted with a large platinum sheet of size 15×20×2mm as a counter electrode (CE), saturated Ag/AgCl electrode as a reference electrode (RE) and Ti or its alloy as the working electrode (WE). The impedance diagrams were recorded at the free immersion potential (OCP) by applying a 10 mV sinusoidal potential through a frequency domain from 100 kHz down to 100 mHz.

The EIS was recorded after reading a steady state open-circuit potential. The polarization scans were carried out at a rate of 1 mV/s. Corrosion current,  $i_{\text{corr}}$ , which is equivalent to the corrosion rate is given by the intersection of the Tafel lines extrapolation. Open circuit potential, Polarization and Electrochemical impedance spectroscopy (EIS) measurements were carried out using an electrochemical workstation IM6e Zahner-electrik GmbH, Meßtechnik, Kronach, Germany.

### 3. RESULTS AND DISCUSSION

#### 3.1. Effect of Phosphoric Acid Concentration

##### 3.1.1. Open circuit potential

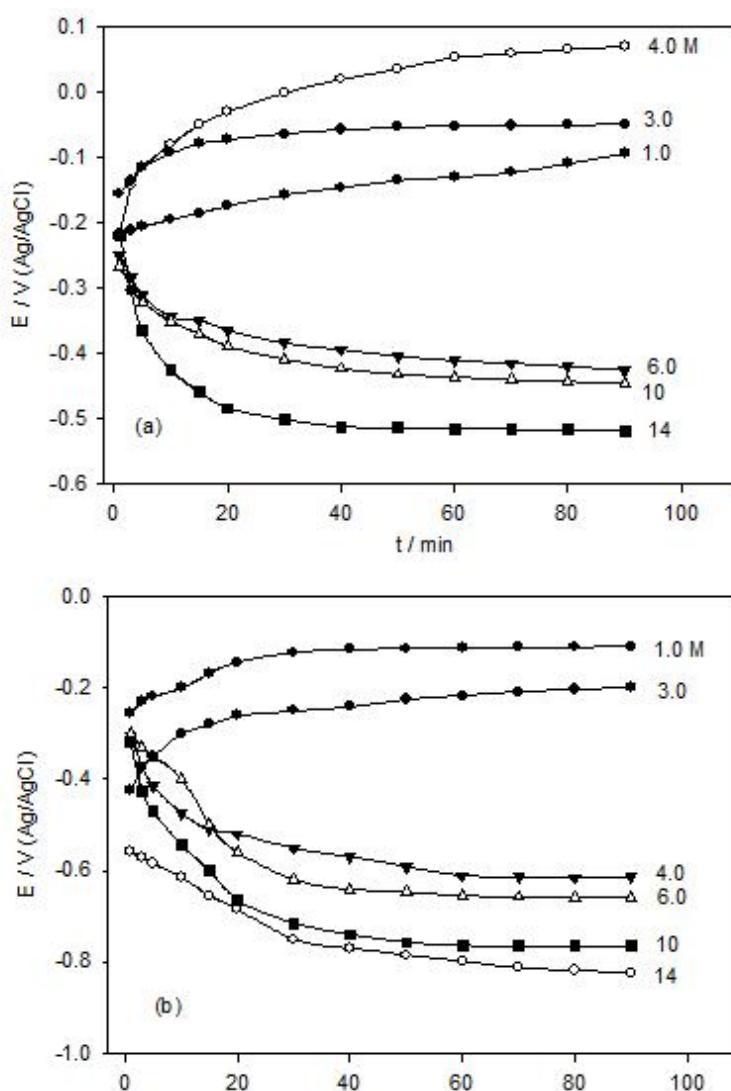


**Figure 1.** Variation with time of the open-circuit potential of (a) Ti and (b) TA6V alloy in H<sub>3</sub>PO<sub>4</sub> solutions of different concentrations at 298 K.

In aqueous solutions the naturally developed oxide film on the abraded surface (the pre-immersion film) grows, dissolves or both of the two processes may occur simultaneously depending on the electrode type as well as the electrolyte composition. The open circuit potential (OCP) of the mechanically polished (MP) surfaces for titanium and Ti-6Al-4V alloy was followed with time over a period of 90 minutes at 298 K in  $\text{H}_3\text{PO}_4$  solutions of different concentrations. The potential transients shown in Fig. 1 reveal two different types of behavior for titanium and its alloy. In the concentration range 1.0-4.0 M  $\text{H}_3\text{PO}_4$ , the OCP of titanium drifts in the positive direction with time and tends to reach a steady state value that increases with concentration (cf. Fig. 1(a)). However, for Ti-6Al-4V alloy the OCP shifts to more noble values with time in 1.0 to 3.0 M  $\text{H}_3\text{PO}_4$  solution and tends to stabilize around an average value that decreases with concentration as shown in Fig. 1(b). The positive shift in potential could be associated with thickening of the oxide film formed on the material surface while the negative shift is due to its thinning and dissolution. For the higher  $\text{H}_3\text{PO}_4$  concentrations starting from 6.0 M for Ti and 4.0 M for the alloy, the transients measured are all similar in nature, where the potential changing towards more negative values immediately on immersion. This continues until the surface film thins to a degree that it becomes stable with respect to its environment. In any solution, attainment of the stationary potential value ( $E_{ss}$ ) for Ti-6Al-4V alloy is sluggish and is more negative compared to the pure Ti metal. Furthermore, a shift in the potential to more negative values occurs as the acid concentration increases for the two samples.

Singh [23] found that the potential of the Ti-6Al-4V alloy in 85 wt%  $\text{H}_3\text{PO}_4$  as well as in solutions containing low concentrations of water shifts in active direction with time, indicating dissolution of the pre-existing naturally formed oxide film on the alloy surface. However, it has been reported by Robin et al [10] that Ti-4Al-4V alloy obtained from Ti-6Al-4V scrap by melting in an electron furnace, was found to be passive in 20 wt%  $\text{H}_3\text{PO}_4$  and presented an active behavior in 40-80 wt%  $\text{H}_3\text{PO}_4$ . In addition, the present results indicate that for both titanium and Ti-6Al-4V alloy the  $E_{ss}$  values measured in concentrated  $\text{H}_3\text{PO}_4$  solutions (higher than 4.0 M) lie in the active ( $\text{Ti}^{3+}$ ) region on the Pourbaix diagram of the Ti- $\text{H}_2\text{O}$  system, whereas in solutions with concentrations  $\leq 4.0$  M for Ti or  $\leq 3.0$  M for Ti-6Al-4V alloy, the obtained  $E_{ss}$  values are in the passive ( $\text{TiO}_2$ ) region [24].

### 3.1.2. Impedance measurements

Electrochemical impedance spectroscopy (EIS) is a technique for studying the spontaneous passivation of metals in electrolytes, various oxide films on metal surfaces have been characterized by this technique. The EIS data of Ti and Ti-6Al-4V surfaces were examined in order to establish the peculiar corrosion behavior of these two samples relative to each other in phosphoric acid solutions over a wide concentration range (1.0-14 M). All the impedance measurements were collected in the frequency range of  $10^5$ - $10^{-1}$  Hz at 298 K. Prior to each experiment the sample was left immersed in the respective concentration of the acid for about 90 minutes until a stabilized potential was reached. The experimental impedance results for titanium and Ti-6Al-4V samples are displayed in Fig. 2(a- b) as the Bode format of logarithm the impedance modulus  $|Z|$ , and the phase angle ( $\theta$ ) vs. the logarithm of the frequency ( $f$ ). The Bode plot shows lower resistive region at high frequencies that corresponding to the

solution resistance  $R_s$ , while at low frequencies the resistive arrest can be discerned only at the higher concentrations ( $\geq 6.0$  M).

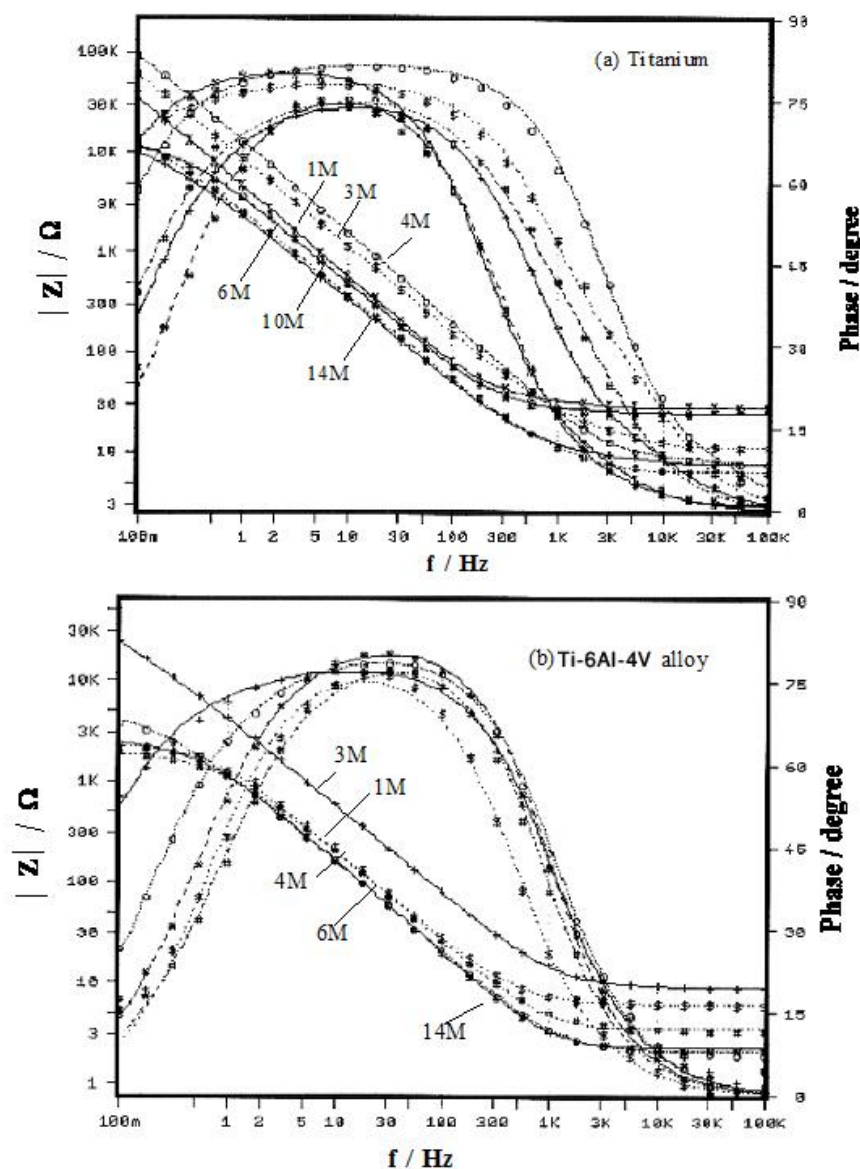


**Figure 2.** Bode plots for (a) titanium and (b) Ti-6Al-4V alloy in phosphoric acid solutions of different concentrations; at 298 K.

The Bode plot shows also a broad phase maximum at intermediate frequencies at the lower  $H_3PO_4$  concentration indicating the formation of a more thick protective film and a somewhat narrow phase maximum with increasing  $H_3PO_4$  concentration especially for Ti-6Al-4V alloy reflecting the formation of less protective film [25]. According to the literature [26-28] the film on Ti alloys is composed of a bi-layer consisting of a porous outer layer and a barrier like inner layer.

It has been established that the impedance characteristics of a metal/solution interface is well simulated by a simple circuit model (Randle's cell) consisting of a parallel combination of a capacitor

( $C_{dl}$ ) and a resistor ( $R_{ct}$ ) with an additional series resistance corresponding to the solution resistance ( $R_s$ ). The impedance spectra obtained experimentally were analyzed using Thales software provided with the electrochemical workstation.

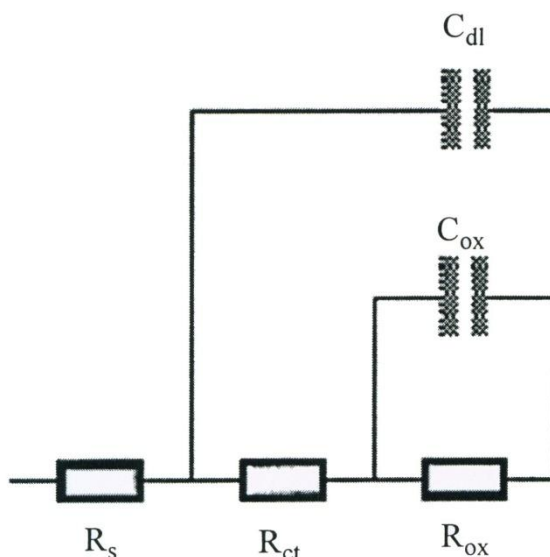


**Figure 3.** Equivalent circuit used to fit the experimental impedance data for an electrode/electrolyte solution interface, where :  $R_s$  = solution resistance;  $R_{ct}$  = charge transfer resistance;  $R_{ox}$  = surface oxide film resistance;  $C_{dl}$  = double layer capacitance in terms of CPE;  $C_{ox}$  = oxide film capacitance in terms of CPE

The data were found to be adequately fitted to the equivalent circuit given in Fig. 3 where another  $R_{ox}C_{ox}$  parallel combination was introduced to the simple Randle's cell to account for the presence of surface oxide film.

Instead of pure capacitors, constant phase elements (CPE) were introduced which can be related to a distribution of the relaxation times as a result of different degrees of surface inhomogeneity, roughness effects and variation of surface layers composition [29]

The impedance associated with the capacitances of the oxide layers is described by the complex frequency dependent impedance ( $Z_{CPE}$ ) defined as [30-32].

$$Z_{CPE} = \frac{1}{Q(j\omega)^x} \text{----- (1)}$$

where  $Q$  is the frequency-independent real constant of the CPE which is identical to the idealized capacitance ( $C_{ox}$ ) at  $\omega = 1$ ,  $\omega$  being the angular frequency ( $\omega = 2\pi f$ ),  $f$  is the frequency and  $j$  is  $\sqrt{-1}$ . The value of  $x$  can vary between 1 for a perfect capacitor and -1 for a perfect inductor. In all cases, good conformity between theoretical and experimental was obtained for the whole frequency

range with an average error of 3%. The experimental values are correlated to the theoretical impedance parameters of the equivalent model. The calculated equivalent circuit parameters for titanium and its alloy are presented in Table 1.

**Table 1.** Equivalent circuit parameters for Ti and Ti-6Al-4V alloy as a function of H<sub>3</sub>PO<sub>4</sub> concentration at 298 K.

Electrode	[H <sub>3</sub> PO <sub>4</sub> ] / M	R <sub>ox</sub> /	C <sub>ox</sub> /	x	R <sub>ct</sub> /	C <sub>dl</sub> /	R <sub>s</sub> /
		kΩ cm <sup>2</sup>	μF cm <sup>-2</sup>		Ω cm <sup>2</sup>	μF cm <sup>-2</sup>	
Ti	1.0	90.39	22.32	0.83	1.61	59.38	28.52
	3.0	105.10	19.50	0.86	2.92	33.32	9.34
	4.0	113.42	17.11	0.87	4.01	18.48	7.77
	6.0	4.01	57.59	0.79	2.51	41.79	6.39
	10	2.95	82.62	0.82	0.73	46.20	7.64
	14	2.57	90.21	0.85	0.464	51.31	24.75
Alloy	1.0	20.10	20.22	0.80	1.43	135.57	8.77
	3.0	24.80	18.52	0.80	1.10	155.10	7.17
	4.0	1.75	27.84	0.66	0.98	205.78	1.78
	6.0	0.89	34.89	0.77	0.37	221.26	2.22
	10	0.47	40.09	0.77	0.29	251.35	3.40
	14	0.30	43.36	0.77	0.15	275.46	6.08

The value of the exponent *x* derived from the best fit of the EIS data lie between 0.79-0.87 for the pure Ti and between 0.66-0.80 for the alloy, which points to higher surface homogeneity for the passive oxide film on the titanium metal than on its alloy. Both *x* and the other circuit parameters were found to be concentration dependent. The change in the oxide layer capacitance (C<sub>ox</sub>) can be used as an indicator for the change in this layer thickness (d). The reciprocal capacitance (1/C<sub>ox</sub>) of the passive layer is directly proportional to its thickness in accordance with the equation:

$$1/C_{ox} = d / (\epsilon_o \epsilon_r A) \text{----- (2)}$$

where  $\epsilon_r$  is the relative dielectric constant of the oxide film,  $\epsilon_o$  being the permittivity of vacuum ( $8.85 \times 10^{-12} \text{ F cm}^{-1}$ ) and A is the electrode area in  $\text{cm}^2$ . Although the actual value of  $\epsilon_r$  within the film is difficult to estimate, a change of C can be used as an indicator for change in the film thickness (d) [33]. Hence the reciprocal capacitance (1/C) is directly proportional to oxide film thickness [34,35].

Figs. 4 and 5 show respectively, the variation of the relative thickness (1/C<sub>ox</sub>) and the resistance (R<sub>ox</sub>) of spontaneously formed (currentless) passive films on the two sample surfaces with H<sub>3</sub>PO<sub>4</sub> concentration in the range from 1.0 M to 14.0 M. The results of 1/C<sub>ox</sub> and R<sub>ox</sub> seem to be consistent with each other, where titanium exhibits oxide film thickening in the low concentration range from 1.0 to 4.0 M H<sub>3</sub>PO<sub>4</sub> solutions, while the alloy thickening range extends only to 3.0 M H<sub>3</sub>PO<sub>4</sub>.

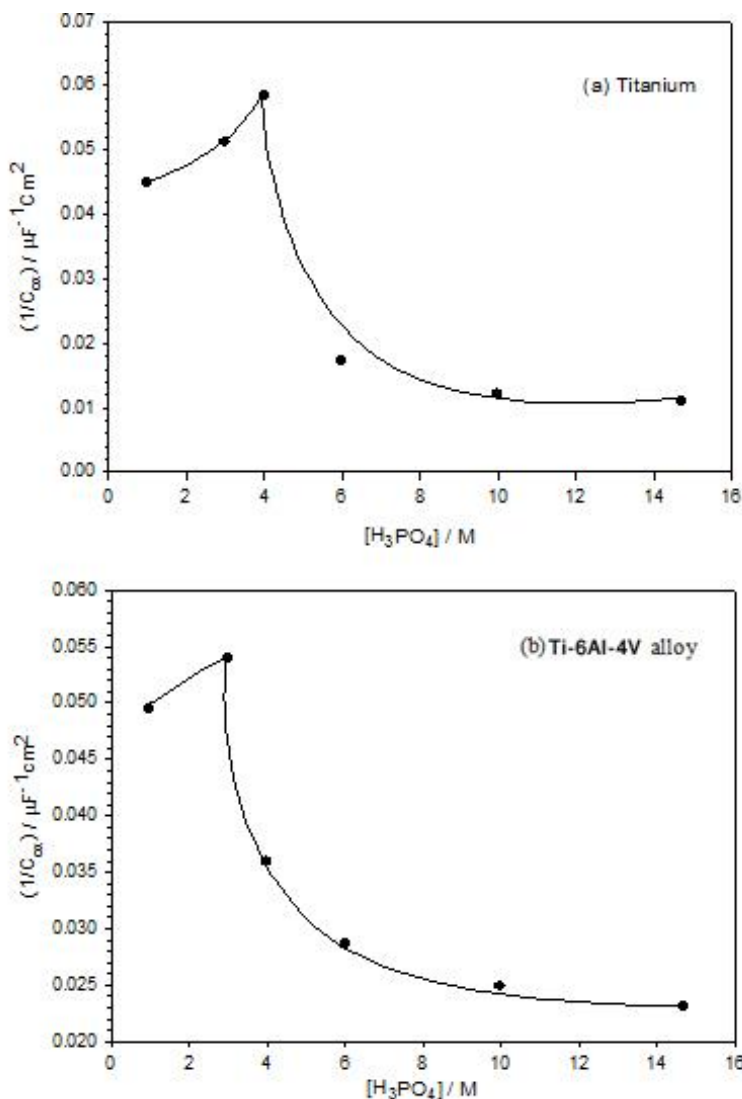


**Figure 4.** Relative thicknesses of spontaneously formed passive films on (a) Ti and (b) Ti-6Al-4V alloy as a function of H<sub>3</sub>PO<sub>4</sub> concentration; at 298 K.

A spontaneous passive-active transition at acid concentration of 4.0 M for Ti and at 3.0 M for Ti-6Al-4V sample was found to occur where the values of  $1/C_{ox}$  (Fig. 4) as well as  $R_{ox}$  (Fig. 5) decrease sharply at first and then more slowly with further increase in the acid concentration tending to reach a lower stationary thickness with a smaller resistance of about 2500 and 300 Ω for Ti and Ti-6Al-4V alloy, respectively. This behavior indicates activation and thinning due to dissolution of the passive oxide film on the sample surfaces as the corrosiveness of the test medium is increased. The dissolution reaction for the oxide film on pure Ti in acid solution might be written as:



In addition to this reaction, possible dissolution of any alumina (Al<sub>2</sub>O<sub>3</sub>) within the passive film on the Ti-6Al-4V alloy surface may also dissolve at open circuit via the reaction [36]:



The results reveal in general that, although the alloy possesses stationary  $1/C_{\text{ox}}$  value about double that for its base metal, yet its resistance is almost 1/8 times the resistance of the Ti oxide film.

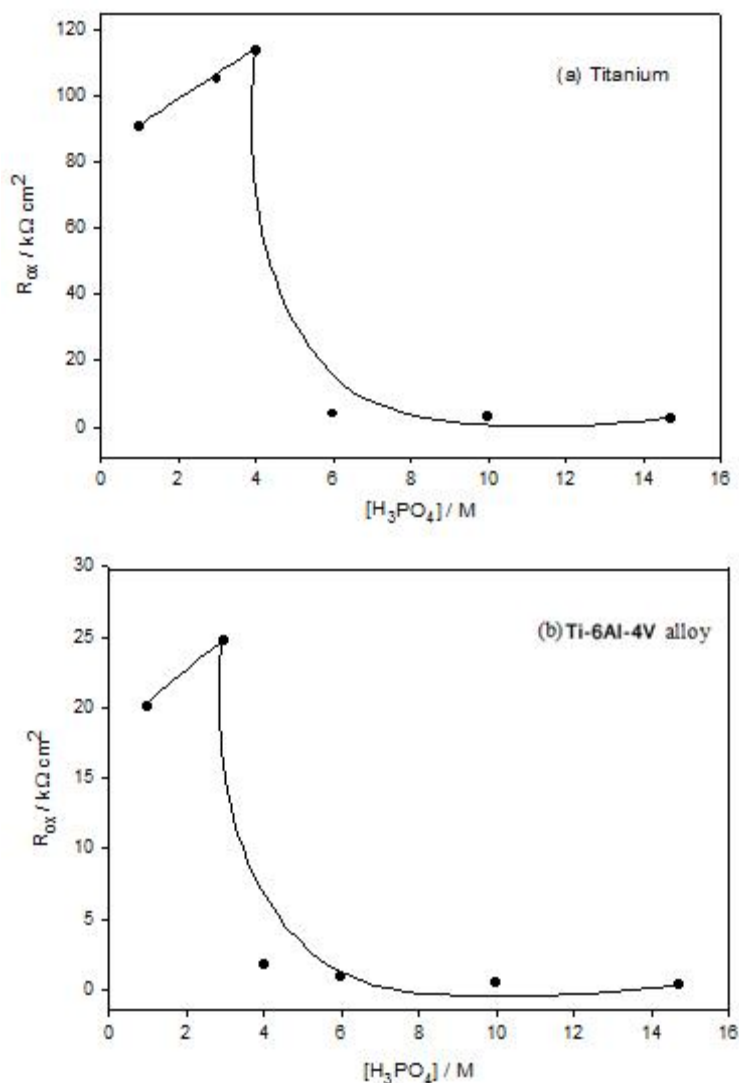


**Figure 5.** Resistance ( $R_{\text{ox}}$ ) of spontaneously formed passive films on (a) Ti and (b) Ti-6Al-4V alloy as a function of  $\text{H}_3\text{PO}_4$  concentration; at 298 K.

This can be attributed to the presence of much more surficial defects in the oxide of the alloy compared with that for the pure Ti metal. The diminish of these surficial defects in the oxide films on Ti makes them more compact and therefore highly resistant and exhibiting better protection against corrosion. It is clear that the results obtained from the analysis of the EIS data are consistent with the OCP measurements which show that pure titanium is more corrosion resistant than its alloy at any given  $\text{H}_3\text{PO}_4$  concentration.

3.2. Effect of Temperature

3.2.1. Polarization behavior

The influence of temperature on the corrosion rate of Ti and Ti-6Al-4V alloy was conducted in 1.0 M H<sub>3</sub>PO<sub>4</sub> solution over the temperature range 288-328 K using the potentiodynamic polarization measurements at scan rate of 1mVs<sup>-1</sup>. Titanium and its alloy show a broadly similar polarization curves at the different temperatures which suggest similar reactions at the surface of the electrode but with different rates.

Generally, the corrosion current densities *i*<sub>corr</sub> for Ti and Ti-6Al-4V alloy is found to increase with the increase in temperature showing that the surface film on each sample becomes less resistant to corrosion at higher temperatures, probably due to acceleration in the film dissolution rate. Degradation of the surface oxide film through thermal activation suggests that the corrosion process is of a purely chemical nature. Furthermore, the values of *i*<sub>corr</sub> observed at any given temperature were higher for the alloy as compared to its base metal, indicating that pure Ti is less susceptible to corrosion than its alloy at identical experimental conditions.

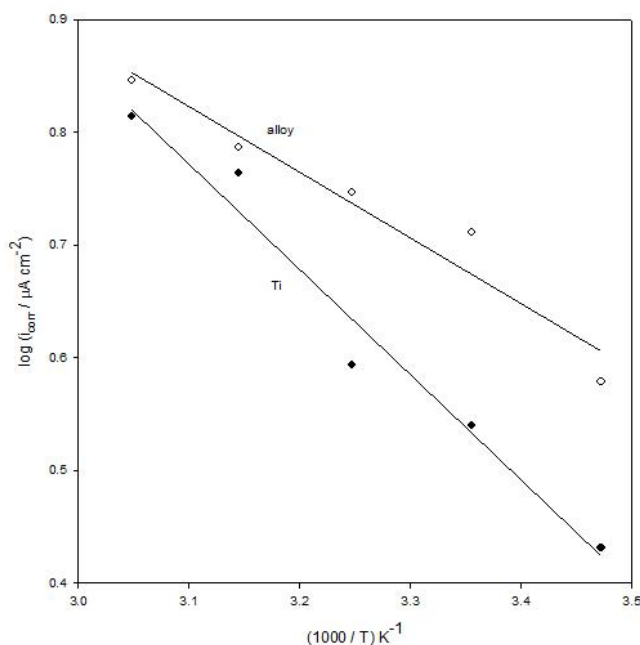


**Figure 6.** Arrhenius plots for the effect of temperature on the corrosion current density of Ti and Ti-6Al-4V alloy in 1.0 M H<sub>3</sub>PO<sub>4</sub> solution.

A plot of the corrosion rate, which is represented by the corrosion current density (*i*<sub>corr</sub>) versus 1/T obeys the familiar Arrhenius equation [37].

$$\log i_{corr} = constant - \left(\frac{E_a}{2.303R}\right) \frac{1}{T} \dots\dots\dots (5)$$

The Arrhenius plots for the two investigated samples in 1.0 M H<sub>3</sub>PO<sub>4</sub> solution are displayed in Fig. 6. The apparent activation energies ( $E_a$ ) of the corrosion process estimated from these plots for the metal and its alloy are 17.90 and 11.10 kJ mol<sup>-1</sup>, respectively. The somewhat higher values reported recently by Mogoda et al [38] for the corrosion process of Ti and Ti-6Al-4V alloy in H<sub>2</sub>SO<sub>4</sub> and HCl solutions indicate that the two samples are comparatively more corrosive in phosphoric acid than in the other reducing acids (H<sub>2</sub>SO<sub>4</sub> and HCl). Dissolution of the oxide film is strongly influenced by its solid state properties and consequently by its conditions of formation. Hence, the present values of  $E_a$  estimated at the free corrosion potential are in agreement with the previous observation [39], where it was found that the dissolution rate is the highest for the oxide film formed on Ti in H<sub>3</sub>PO<sub>4</sub> among the ones formed in H<sub>2</sub>SO<sub>4</sub> or HCl solutions. The dependence of the corrosion behavior on the type of the acid can be ascribed to the participation of PO<sub>4</sub><sup>3-</sup> ion in the dissolution reaction as well as in surface modification [8].

### 3.2.2. Open circuit potential

The effect of temperature on the electrochemical properties of the native passive oxide film on Ti surface relative to that of its Ti-6Al-4V alloy was also investigated in 1.0 M H<sub>3</sub>PO<sub>4</sub> solution. For this purpose, the time dependence of the OCP was followed over a period of 120 minutes at different temperatures ranging from 288 to 328 K, until steady state ( $E_{ss}$ ) values were reached. Fig. 7(a- b) shows that for both Ti and Ti-6Al-4V electrodes the trend at all temperatures is for OCP to become more positive with time due to oxide film healing and growth. On the other hand, there is negative shift of the whole potential transient with raising the temperature.

More information can be extracted by considering the variation of the OCP ( $E$ ) with the logarithm of immersion time ( $\log t$ ). There is a linear relation between  $E$  and  $\log t$  following the equation [40]:

$$E = \text{constant} + 2.303 (\delta/B) \log t \quad (6)$$

where  $\delta$  is the rate of oxide film thickening per decade of time and  $B$  is a constant. where the slope of the plot is directly proportional to the rate of oxide film thickening ( $\delta$ ). Over the temperature range studied, there is an inflection observed in each graph. This seems to reflect the dual nature of the spontaneously growing oxide film, i.e. it consists of two layers having different growth rates [39]. The inner layer is always with a higher rate of thickening ( $\delta_1$ ) and it can be considered as a continuation of the native pre-immersion oxide film. After a longer immersion periods a second type of layer with a lower rate of thickening ( $\delta_2$ ) is formed on the surface of the first one. The results in Table 2 indicate that at any given temperature the two thickening rates are always greater for Ti than for its alloy. These results imply that the degree of self passivation of Ti-6Al-4V alloy in phosphoric acid solution is much inferior to that of its base metal pure titanium.

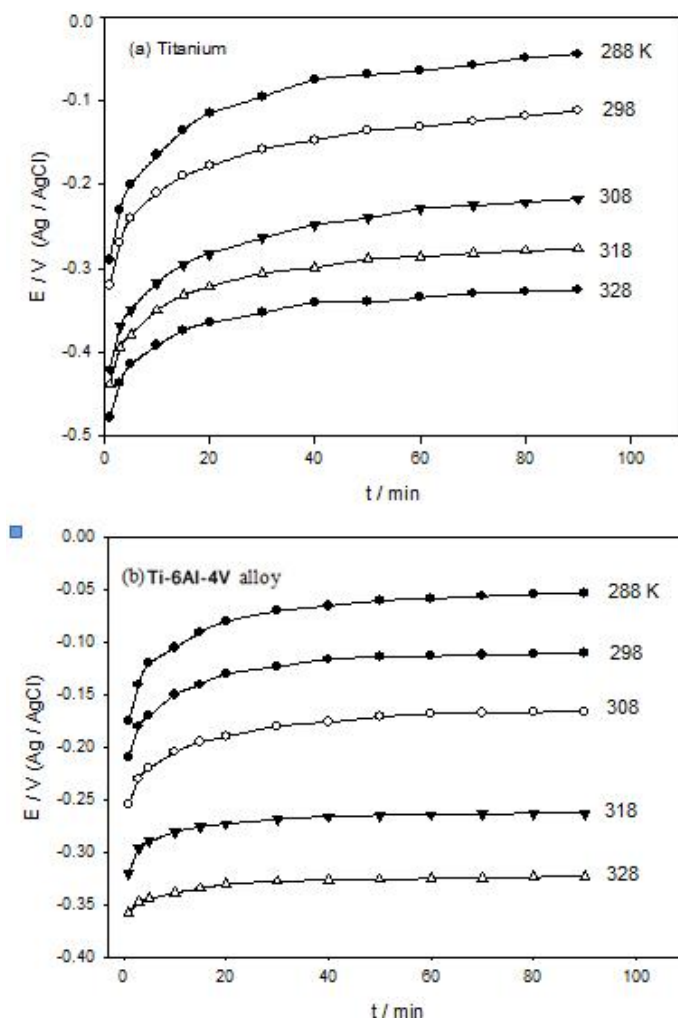


**Figure 7.** Variation with time of the open circuit potential of (a) Ti and (b) Ti-6Al-4V alloy in 1.0 M H<sub>3</sub>PO<sub>4</sub> solution at different temperatures.

**Table 2.** Thickening rates  $\square_1$  and  $\square_2$  (in nm / decade) for the inner and the outer layers of the spontaneous passive films on Ti and Ti-6Al-4V alloy surfaces as a function of temperature in 1.0 M H<sub>3</sub>PO<sub>4</sub>.

Electrode	T / K	$\square_1$ / nm decade-1	$\square_2$ / nm decade-1
Ti	288	1.82	1.72
	298	1.79	1.63
	308	1.62	1.46
	318	1.49	1.02
	328	1.44	0.95
Alloy	288	1.20	0.56
	298	1.00	0.28
	308	0.84	0.20
	318	0.56	0.17
	328	0.34	0.16

3.2.3. EIS measurements

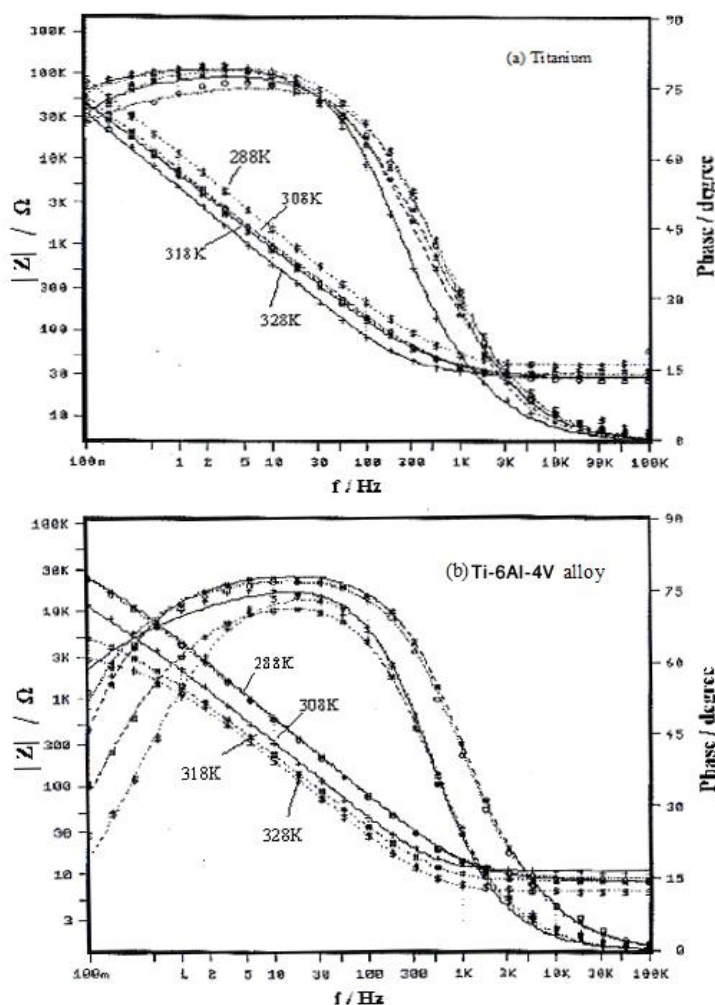


**Figure 8.** The Bode plots in 1.0 M  $H_3PO_4$  solution at different temperatures for (a) Ti and (b) Ti-6Al-4V alloy.

To confirm further the OCP results, impedance spectroscopy (IS) was examined in 1.0 M  $H_3PO_4$  solution as a function of temperature. The ac impedance response of titanium and its Ti-6Al-4V alloy was recorded after the OCP had reached its steady state value at fixed temperature in the range from 288 to 328 K as shown in Fig. 8(a- b). The impedance data of the two samples were analyzed using the same equivalent circuit shown in Fig. 3 since only one phase lag -broad for Ti and narrow for Ti-6Al-4V is seen in Fig. 8(a- b), the time constant of the passive oxide ( $R_{ox}-C_{ox}$ ) circuit is tentatively assumed to be much greater than that for the double layer, implying that the EIS data is dominated by the surface oxide film. The calculated fitting parameters showed that the values of  $R_{ox}$  as well as  $R_{ct}$  for titanium are higher than those for the alloy. This is due to the higher thickening rate of the oxide film on titanium compared to its alloy as observed before from the OCP results. The variation of the relative oxide film thickness ( $1/C_{ox}$ ) as well as its resistance ( $R_{ox}$ ) with temperature for titanium and its

alloy are shown in Fig. 9(a- b), where both parameters decrease linearly with the temperature regardless of the sample nature.

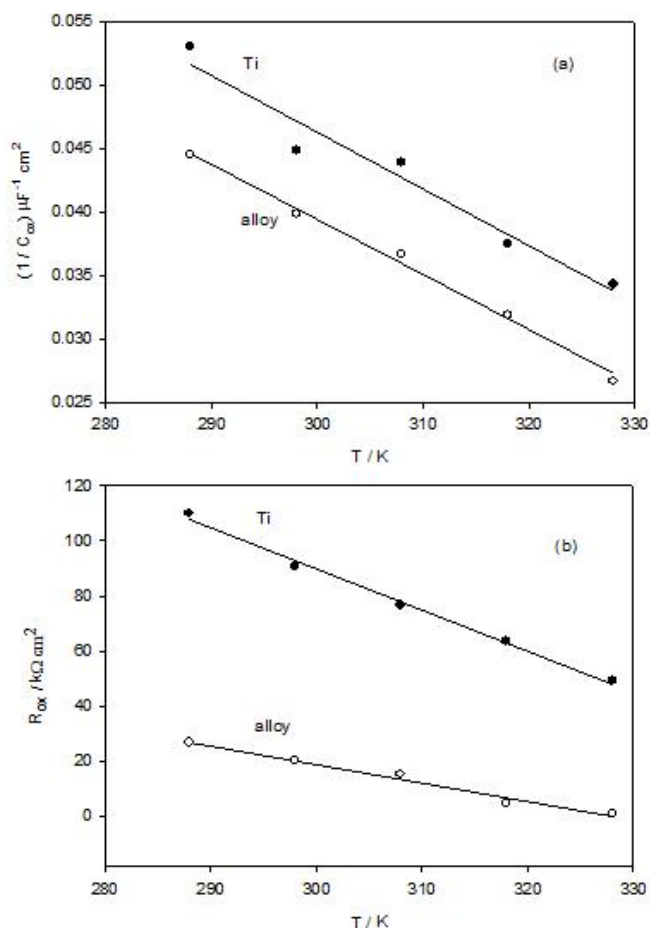


**Figure 9.** (a) The relative thickness ( $1/C_{ox}$ ) and (b) the resistance ( $R_{ox}$ ) of spontaneously formed passive films in 1.0 M  $H_3PO_4$  solution at different temperatures.

This indicates that the growth of the spontaneously formed oxide film on the two substrates decreases as the solution temperature is raised. Primarily, the temperature may enhance the dissolution of the oxide film in acid media as can be substantiated from the increase in the corrosion intensity ( $i_{corr}$  value) of the two samples described before. In general, the results indicate that lowering the solution temperature favors the formation of a thicker oxide film offering better protection for both titanium and Ti-6Al-4V alloy in phosphoric acid medium.

#### 4. CONCLUSIONS

1- The thickness of the native oxide film formed on Ti and Ti-6Al-4V alloy increases with increasing  $H_3PO_4$  concentration up to 4.0 and 3.0 M for Ti and its alloy respectively, and then it decreases for higher acid concentrations.

2- The values of the corrosion current density  $i_{\text{corr}}$  at any given temperature are higher for the alloy as compared to those for the metal.

3- The apparent activation energies of the corrosion process for Ti and Ti-6Al-4V are 17.90 and 11.10 kJ mol<sup>-1</sup>, respectively.

At any given temperature, titanium exhibits higher thickening rate for its oxide film growth in 1.0 M H<sub>3</sub>PO<sub>4</sub> medium.

1. ASM Metals Handbook, vol. 2, 10th edition, Materials Park, Ohio, USA, 1990, pp. 586–591.
2. J. K. Wessel, The Handbook of Advanced Materials, Wiley Interscience, Oak Ridge, Tennessee, USA, 2004, pp. 272–319.
3. S. Luiz de Assis, S. Wolyneq, I. Costa, *Electrochim. Acta* 51 (2006) 1815.
4. R.W. Shutz, D.E. Thomas, ASM Metals Handbook, Corrosion, vol. 13, ninth ed., ASM International, Metals Park, OH, 1987, p. 669.
5. T. Ohtsuka, M. Masuda, N. Sato, *J. Electrochem. Soc.* 132 (1985) 787.
6. T. Shibata, Y. Zhu, *Corros. Sci.* 37 (1995) 253.
7. R. Narayanan, S.K. Seshadri, *Corros. Sci.* 50 (2008) 1521.
8. V. B. Singh, S. M. A. Hosseini, *Corros. Sci.* 34 (1993) 1723.
9. V. B. Singh, S. M. A. Hosseini, *J. Appl. Electrochem.* 24 (1994) 250.
10. A. Robin, J. L. Rosa, H. R. Z. Sandim, *J. Appl. Electrochem.* 31 (2001) 455.
11. V. B. Singh, A. Gupta, *J. Appl. Electrochem.* 32 (2002) 795.
12. S. Ferdjani, D. David, G. Beranger, *Journal of Alloys and Compounds* 200 (1993) 191.
13. E. Krasicka-Cydzik, *Corros. Sci.* 46 (2004) 2487.
14. N. D. Tomashov, G. P. Chernova, Yu. S. ruscol and G. A. Ayuyan, *Electrochim. Acta* 19 (1974) 159.
15. M. Metikos-Hukovic, A. Kwokal, J. Piljac, *Biomaterials* 24 (2003) 3765.
16. C. E. B. Marino, S. R. Biaggio, R. C. Rocha-Filho and N. Bocchi, *Electrochim. Acta* 51(2006) 6580.
17. A. M. Fekry, *Electrochim. Acta* 54 (2009) 3480.
18. F. El-Taib Heakal, Kh. A. Awad, *Int. J. Electrochem. Sci.*, 6 (2011) 6483.
19. A.K. Shukla, R. Balasubramaniam, S. Bhargava, *Intermetallics* 13 (2005) 631.
20. N. A. Al-Mobarak, A. M. Al-Mayouf, A. A. Al-Swayih, *Material Chemistry and Physics* 99 (2006) 333.
21. B. Grosogeat, M. Boint, F. Dalard, M. Lissac, *Biomedical Materials and Engineering* 14 (2004) 323.
22. F. El-Taib Heakal, A. A. Ghoneim, A. S. Mogoda, Kh. Awad, *Corros. Sc.*, 53 (2011) 2728.
23. D. D. N. Singh, *J. Electrochem. Soc.* 132 (1985) 378.
24. M. Pourbaix, "Atlas of Electrochemical Equilibrium in Aqueous Solutions", NACE Pub., Houston, TX. p. 213 (1974).
25. K. M. Ismail and W. A. Badawy, *J. Appl. Electrochem.* 30 (2000) 1303.
26. R.M. Souto, M. M. Laz, R. L. Reis, *Biomaterials* 24 (2003) 4213.
27. R.Venugopalan, J. J. Weimer, M.A. George, L.C. Lucas, *Biomaterials* 21 (2000) 1669.
28. A. M. Fekry, Rabab M. El-Sherif, *Electrochim Acta* 54 (2009) 7280.
29. C. Fonseca, M. A. Barbosa, *Corrosion Sci.* 43 (2001) 547.
30. F. El-Taib Heakal, A. M. Fekry, A. A. Ghoneim, *Corrosion Sci.* 50 (2008) 1618.
31. M. A. Ameer, A. M. Fekry, A. A. Ghoneim, *Corrosion* 65 (2009) 587.
32. K. Juttner, *Electrochim. Acta* 35 (1990)1501.
33. M. A. Ameer, A. A. Ghoneim, F. Heakal and A.M. Fekry, *Surface and Interface Analysis* 42 (2010) 95.

34. J. S. Leach, B. R. Pearson, *Electrochim. Acta* 29 (1984) 1271.
35. F. El-Taib Heakal, A. S. Mogoda, A. A. Mazhar, M. S. El-Basiouny, *Corrosion Sci.* 27 (1987) 453.
36. A. A. Mazhar, F. El-Taib Heakal, A. S. Mogoda, *Corrosion*, 44 (1988) 354.
37. P. W. Atkins, "Physical Chemistry", 5th ed., 877, Oxford University Press, Oxford, UK (1994).
38. A. S. Mogoda, Y. H. Ahmed, W. A. Badawy, *J. Appl. Electrochem.* 34 (2004) 873.
39. F. El-Taib Heakal, A. S. Mogoda, A. A. Mazhar and M. S. El-Basiouny, *Corros. Sci.* 27(1987) 453.
40. J. M. Abd El Kader and A. M. shams El Din, *Br. Corros. J.* 14 (1979) 40.